

PHYSICAL REVIEW C

NUCLEAR PHYSICS

THIRD SERIES, VOL. 2, NO. 6

DECEMBER 1970

Thermonuclear-Reaction Rates at High Temperature*

Georges Michaud† and William A. Fowler

California Institute of Technology, Pasadena, California 91109

(Received 4 May 1970)

Thermonuclear-reaction rates have been calculated over the temperature range $2 \leq (T/10^9)^{\circ}\text{K} \leq 6$ for some cases of particular interest in nucleosynthesis during silicon burning (Michaud and Fowler). We explicitly relate our calculations to the evaporation theory and the optical model for particle channels. For γ -ray channels we develop an approximate formula fitted to the experimental results of Macklin and Gibbons on radiative capture reactions for neutrons. We compare our calculated rates with available data and discuss the effect of excited states.

I. INTRODUCTION

Astrophysical calculations currently being undertaken require a large number of nuclear-reaction rates. Many of these reactions proceed through a compound nucleus and at sufficiently high energy such that *many* resonances lie in the effective energy interval determined by the product of the barrier penetration factor and the Maxwell-Boltzmann factor. For these reactions, the Woods-Saxon potential represents reasonably well the nuclear physics involved in the particle channels. However, a different approach is needed for the photon channel.

In what follows, we explicitly relate our calculations of the particle reactions to the optical model with a Woods-Saxon potential. For the γ -ray channels, we develop a semiempirical formula. The free parameters in this formula are evaluated by comparison with the experimental results of Macklin and Gibbons^{1,2} on the radiative capture of neutrons. Some nuclear-reaction rates which have been measured and some which are used in calculations on nucleosynthesis during silicon burning³ are then calculated.

The uncertainties involved are discussed briefly: Uncertainties of a factor of 2 are found in the nucleon channels, of 5 in the α -particle channels (or perhaps more owing to uncertainties in the applicability of the optical model as discussed in

Michaud, Scherk, and Vogt⁴), and of 5 in the γ -ray channel. These uncertainties are not compounded in most cases, since one of the reaction channels usually dominates in the decay of the compound nucleus, and the over-all reaction-rate uncertainty is approximately equal to that in the weaker channel.

II. PARTICLE CHANNELS

We now relate our calculations of particle channels to the experimental parameters through the evaporation theory and the optical model (with Woods-Saxon potentials). We start from the results of the evaporation theory for reaction cross sections averaged over the resonances of the compound nucleus⁵:

$$\bar{\sigma}_{\alpha\alpha'} = \frac{\pi}{k_{\alpha}^2} \sum_{J^{\pi}} \frac{2J+1}{(2I+1)(2i+1)} \left[\sum_{s,i} T_i(\alpha) \right] \times \left[\sum_{s',i'} T_{i'}(\alpha') / \sum_{\alpha''s''i''} T_{i''}(\alpha') \right], \quad (1)$$

where a represents a pair of particles and their state of excitation, I and i are the intrinsic spins of the initial pair of interacting particles, s is the channel spin, l the orbital angular momentum of the pair, and J^{π} is the angular momentum and parity of the compound nucleus. The vector sums $\vec{s} = \vec{I} + \vec{i}$ and $\vec{J} = \vec{l} + \vec{s}$ must be consistent with the con-

servation laws for angular momentum and parity. The unprimed quantities refer to the incoming channel, the primed quantities refer to the outgoing channel, and the double-primed quantities should be summed over all open channels in the compound nucleus, including excited states of the residual nuclei. It is assumed that all $T_{s_i}(\alpha) = T_i(\alpha)$, and similarly in the primed and double-primed cases.

For particle channels, the $T_i(\alpha)$'s can be obtained through the optical model with Woods-Saxon potentials:

$$V_{\text{WS}}(r) = (V_0 + iW_0)/(1 + e^{(r-R_0)/a}), \quad (2)$$

where a is the surface thickness, R_0 is the radius of the well, and V_0 and W_0 are the real and imaginary parts of the potential close to $r=0$ (since $R_0 \gg a$). For a justification and a detailed discussion of the optical model, the Woods-Saxon potential and the equivalent square well, see Michaud, Scherk, and Vogt.⁴ The calculations are simplified if one uses the equivalent square well defined by

$$\begin{aligned} V &= V_1 + iW_1, & r < R_1, \\ V &= 0, & r \geq R_1, \\ R_1 &= R_0 + \Delta R, \\ W_1 &\simeq W_0, \end{aligned} \quad (2')$$

and V_1 determined from

$$V_0 R_0^2 \simeq V_1 R_1^2. \quad (2'')$$

The value of ΔR is given by Michaud, Scherk, and Vogt.⁴

Using the equivalent square well to replace the Woods-Saxon potential, the transmission function can be written

$$T_i = \tau_i / (1 + \frac{1}{4}\tau_i)^2, \quad (3)$$

$$\tau_i = 4\pi P_i s_i f, \quad (4)$$

where $P_i = [k r / (F_i^2 + G_i^2)]_{R_1}$ and s_i are the usual square-well nuclear penetrability evaluated at R_1 and strength functions, respectively, and where f is the reflection factor. F_i and G_i are regular and irregular Coulomb wave functions. We have used

the black-nucleus strength function throughout, $s_i = (\pi K R_1)^{-1}$, where $K \approx 1.5A^{1/2} \text{ F}^{-1}$ is a wave number appropriate to the nuclear interior, and A is the reduced atomic mass of the interacting particles. Vogt⁶ has shown that, on the average for neutrons, the black-nucleus strength function multiplied by the reflection factor should be equal to the Woods-Saxon strength function. The same is true for protons. For ⁴He projectiles, the black-nucleus strength function multiplied by f is equal to the diffuse well strength function, since the large W_0 used for ⁴He smooths out any "giant," "shape," or "size" resonance effects. Finally, in the denominator of Eq. (3) we have neglected terms like PR^∞ , SR^∞ , and πSs .⁷ The terms containing R^∞ will be, on the average, zero. They will change sign at resonance. For α particles, they will always be zero, since the large size of W_0 guarantees no resonance effects. For protons and neutrons, numerical calculations prove them to be small. The $\pi S_i s_i$ term is also small. It is zero at a giant resonance, since S_i is zero there (see Vogt⁶). Away from a giant resonance, s_i becomes small by definition of a giant resonance. Using the black-nucleus strength function to calculate $\pi S_i s_i$ then gives an overestimate. Even then, numerical calculations have shown that the $\pi S_i s_i$ term would contribute less than 5% to the value of the denominator in Eq. (3).

We have calculated the transmission function for all particle channels using the square wells equivalent to the Woods-Saxon wells with the parameters indicated in Table I. For $T(\gamma)$, we have used

$$T(\gamma) = 2\pi \Gamma_\gamma / D, \quad (5)$$

where Γ_γ / D is obtained from the semiempirical formula now to be developed. Γ_γ is the radiative width and D is the level separation.

III. γ -RAY CHANNELS

A. Transition Probability and Level Separation

It is assumed that electric and magnetic dipole transitions dominate the radiation widths. Replacing the summation over all transitions from the capturing states to lower states by an integration yields^{8,9}

TABLE I. Parameters of the Woods-Saxon potential [from Michaud, Scherk, and Vogt (Ref. 4) and Vogt (Ref. 5)].

	R_0^a (F)	V_0 (MeV)	W_0 (MeV)	a (F)	ΔR (F)	f
Nucleons	$1.25A_T^{1/3}$	-50	-4	0.5	0.1	2.7
⁴ He	$1.09A_T^{1/3} + 1.6$	-60	-10	0.5	0.7	4.8

^a A_T = atomic mass of the target nucleus.

$$\frac{\Gamma_\gamma(B)}{D(B)} = cR^2 \int_0^B \frac{(B-E)^3}{D(E)} dE, \quad (6)$$

where B is the binding energy in the compound nucleus and is thus approximately equal to the excitation energy for low-energy interactions. The ground state is taken at $E=0$. The radius of the nucleus is designated by R , and c is a constant to be determined empirically in combination with other constants which appear. The R^2 factor is strictly correct only for electric dipole transitions, but no great error is made if magnetic dipole transitions are included in Eq. (6). The main point is that both transitions are proportional to the cube of the transition energy ($B-E$).

Equation (6) requires that the level separation energy $D(E)$ between levels of the same spin and parity in the compound nucleus be specified. In the simplified treatment given here, it is not necessary to include the spin dependence of $D(E)$. Since the dependence of Γ_γ on J is relatively weak, as shown for example in Margenstern, Alves, de Barros, Julien, and Samour,¹⁰ we will later neglect spin and parity conservation in the γ -ray channel. Bethe¹¹ showed that the level separation at excitation energy E for a Fermi gas is given by

$$1/D(E) = c_1(A_C E)^{-2} e^{c_2(A_C E)^{1/2}}, \quad (7)$$

where A_C is the atomic mass of the radiating compound nucleus. For a Fermi gas of neutrons and protons with $R=1.25A_C^{1/3}$ F, the constants in Eq. (7) are given by

$$\begin{aligned} c_1 &= 4.5 \text{ MeV}, \\ c_2 &= 0.57 \text{ MeV}^{-1/2}. \end{aligned} \quad (8)$$

In what follows, c_1 and c_2 are treated as free parameters.

The substitution of Eq. (7) into Eq. (6) yields

$$\frac{\Gamma_\gamma}{D} = \frac{c'_1}{A_C^{10/3}} \int_0^x (X^2 - x^2)^3 x^{-3} e^x dx, \quad (9)$$

where

$$x = c_2(A_C E)^{1/2}, \quad X = c_2(A_C B)^{1/2}, \quad (10)$$

and c'_1 is a new constant proportional to cc_1 .

The integrand of Eq. (9) diverges at $x=0$, but Eq. (7) is not at all correct for $D(E)$ near $E=0$ or $x=0$. It can be shown¹² that if a reasonable lower limit other than zero on the integral in Eq. (9) is chosen and if the integral is evaluated by developing x^{-3} in a series around X , then

$$\frac{\Gamma_\gamma}{D} \approx \frac{48 c'_1}{A_C^{10/3}} e^{x+6/X}. \quad (11)$$

For numerical evaluation this is best expressed as

$$\begin{aligned} \log_{10}(\Gamma_\gamma/D) &= -C_1 - 3.33 \log_{10} A_C + C_2 (A_C B')^{1/2} \\ &+ 1.13 / [C_2 (A_C B')^{1/2}], \end{aligned} \quad (12)$$

where $C_1 \propto c'_1$ and $C_2 = c_2 / \log_{10} e$ are the final constants to be determined empirically. Note that Eq. (8) would indicate $C_2 = 0.25 \text{ MeV}^{-1/2}$. This is to be compared with $C_2 = 0.286 \text{ MeV}^{-1/2}$, as evaluated in what follows. In Eq. (12), B has been replaced by a corrected binding energy B' for the reasons now to be discussed. B' contains additional empirical constants.

B. Excitation Energy

The energy B in Eq. (6) is to be measured from the lowest possible level in a Fermi gas. By hypothesis, in a Fermi gas, there is no interaction between the particles. In the real nucleus, the pairing, deformation, and shell structure effects on the binding energy are ample proof of interaction between the nucleons. In an undeformed nucleus, the pairing and shell-structure effects lower the position of the ground state compared with the excited states. We assume that the most important effect of the deformation is to diminish the correction for the pairing of two of the nucleons. Consequently, if one wants to calculate the level density at an energy B above the ground state of the nucleus, the energy to be used in Eq. (7) should be

$$E = B' = B - \Delta, \quad (13)$$

where Δ is a correction for the pairing, deformation, and shell-structure effects. Thus in Eq. (12), B has been replaced by B' .

In previous work,¹³ Δ was used to take the pairing energy into account. We will also include in Δ the effects of shell structure and of deformation. It allows a convenient and accurate determination of Γ_γ/D .

Figure 1 gives the variation with neutron number of the position of the first excited state in even-even nuclei. We interpret the dashed curve, $\delta(N)$, as giving a measure of the pairing of two nucleons corrected for the effect of the deformation. $\delta(N)$ would be approximately a constant if it were only for pairing, but the correction one must make in the energy due to deformation decreases $\delta(N)$ in the heavy nuclei. (For the sake of brevity we will refer to the dashed curve as giving "the effect of pairing," keeping the effect of deformation implicit, in what follows.) When corrected for the pairing energy, the experimental energies for the first

excited states then give a measure of the energy necessary to break the shell structure. The peaks at $N=20, 28, 50, 82,$ and 126 are apparent in Fig. 1.

The excitation of a nucleus to its first excited state does not require breaking completely the pairing or the shell structure. Rather it is expected that excitation to the first state would require on the average a certain fraction less than unity of the pairing or shell-structure energy. Now an odd-odd nucleus has no pairing effect, and so Δ_{oo} for such a nucleus mainly arises from shell-structure effects, as deformation effects are assumed to be small. Then the excitation energy of the first state of an even-even nucleus E_{ee}^1 , corrected for pairing effects given by $\delta(N)$ from Fig. 1, should be a fraction of Δ_{oo} given by

$$E_{ee}^1 - \delta(N) = (1/C_3) \Delta_{oo}, \quad (14)$$

where $1/C_3$, with C_3 a constant greater than unity, is to be interpreted as the fraction of the shell-structure energy broken on the average in excitation to the first state. For our purposes, we attempt to determine Δ_{oo} empirically from measurements of E_{ee}^1 . To do this, the excitation energies of the first level of the four even-even nuclei bracketing the odd-odd nucleus of interest are used so that

$$\Delta_{oo} = C_3 \left[\sum_{i=1}^4 \frac{1}{4} E_{ee}^1(i) - \delta(N) \right]. \quad (15)$$

In some cases, it is found that $\Delta_{oo} \approx 0$. As an example, $\Delta_{oo} = 1.1$ MeV for ^{50}V is computed from $E_{ee}^1 = 0.98, 1.55, 0.78,$ and 1.43 MeV for $^{48}\text{Ti}, ^{50}\text{Ti}, ^{50}\text{Cr},$ and ^{52}Cr , respectively.

Proceeding in the same manner for an even-odd or odd-even nucleus, one finds

$$\Delta_{eo} = \Delta_{oe} = C_3 \left[\sum_{i=1}^2 \frac{1}{2} E_{ee}^1(i) - \delta(N) \right] + C_4 \delta(N), \quad (16)$$

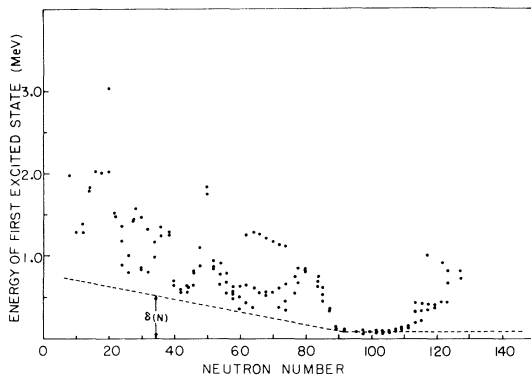


FIG. 1. Excitation energy of the first excited state of nuclei as a function of neutron number. The dashed line gives a measure of the effects of pairing and of deformation.

where the summation is taken over the two even-even nuclei bracketing the nucleus of interest and where $1/C_4$ is interpreted as the fraction of the pairing energy required to excite the first excited state.

For even-even nuclei excitation to the first state breaks only one pair (the paired neutrons or the paired protons). Through $\delta(N)$, the position of the ground state is corrected for the pairing of two nucleons and for the effect of deformation. There remains to correct for the pairing of another two nucleons. This is assumed to bring roughly a constant correction; that is, it is assumed that the deformation is fully taken into account through $\delta(N)$. A constant term C_5 is added to the expression for even-odd or odd-even nuclei:

$$\Delta_{ee} = C_3 [E_{ee}^1 - \delta(N)] + C_4 \delta(N) + C_5, \quad (17)$$

where E_{ee}^1 is the excitation energy of the first excited state of the nucleus of interest. The corrections $\Delta_{oo}, \Delta_{eo}, \Delta_{oe},$ and Δ_{ee} are used where appropriate in Eq. (13) for B' , and thus $C_3, C_4,$ and C_5 appear in Eq. (12) along with C_1 and C_2 when B is properly replaced by B' as has been done.

C. Determination of the Empirical Constants in Γ_γ/D

The empirical constants necessary to determine the average systematic behavior of Γ_γ/D have been determined by comparing the analytical result expressed in Eqs. (12), (13), (15), (16), and (17) with the experimental values of $\langle \sigma v \rangle_T / v_T$ for (n, γ) reactions given by Macklin and Gibbons.^{1,2} Macklin and Gibbons measured $\sigma(n, \gamma)$ for various nuclei over the neutron energy range from ~ 10 to 100 keV and then calculated the Maxwellian-averaged cross section $\langle \sigma v \rangle_T / v_T$ as a function of temperature from $kT = 5$ to 90 keV, using their own and other data. The thermal velocity is found from

$$v_T = (2kT/M_n)^{1/2} = 4.1 \times 10^8 T_9^{1/2} \text{ cm sec}^{-1}, \quad (18)$$

with $T_9 = (T/10^9)\text{K}$.

In order to facilitate the comparison of experiment and theory, we evaluate Eq. (1) for an (n, γ) reaction in the approximation given by Fowler and Hoyle.¹⁴ In this approximation, the over-all statistical weight factor becomes $(2l+1)$ for the l partial wave, and $T_l(n)$ is replaced by $2\pi(\Gamma_n/D)_l$, as well as T_γ by $2\pi(\Gamma_\gamma/D)$ so that

$$\bar{\sigma} = \sum \bar{\sigma}_l, \quad (19)$$

where

$$\begin{aligned} \bar{\sigma}_l &\approx 2\pi^2 \lambda^2 (2l+1) \left[\frac{(\Gamma_n/D)(\Gamma_\gamma/D)}{(\Gamma/D)} \right]_l \\ &\approx 2\pi^2 \lambda^2 (2l+1) \left(\frac{\Gamma_n \Gamma_\gamma}{\Gamma D} \right)_l, \end{aligned} \quad (20)$$

with

$$\frac{\Gamma}{D} = \sum_i \left(\frac{\Gamma}{D} \right)_i \approx \frac{\Gamma_n}{D} + \frac{\Gamma_\gamma}{D}. \quad (21)$$

In most cases considered, only the neutron and γ -ray channels are open. When proton or α -particle channels are open, the charged particles are always well below the Coulomb barrier so that Γ_p/D and Γ_α/D are always much smaller than Γ_n/D , as indicated by the far right-hand side of Eq. (21).

For (n, γ) reactions Eq. (20) is a good approximation, since the neutron channel is the dominant one ($\Gamma_n \gg \Gamma_\gamma$) when it is open and since the angular momentum and parity conservation laws have little effect in the γ -ray channel. The effect of this approximation in other reactions will be discussed below. In Sec. II it was stated that black-nucleus strength functions would be used. This is warranted, since at least two partial waves with differing l values are always involved in our calculations. Overlap of maxima for one partial wave by minima for the other leads to a sum close to that for the smoothly varying black-nucleus value. However, the measurements of Macklin and Gibbons were mainly at lower energy where only one l value, usually $l=0$, contributes substantially. The variation of $(\Gamma_n/D)_{\min l}$ with atomic mass number is then important. In general, we have found that values for $(\Gamma_n/D)_{i=0,1,2}$ are sufficient for our purposes. For $(\Gamma_n/D)_{i=0}$ the experimental values given by Newson¹⁵ for $54 \leq A \leq 208$ have been used. For $(\Gamma_n/D)_{i=1,2}$ the theoretical values of Campbell *et al.*¹⁶ have been used.

From Fowler and Hoyle¹⁴ one has

$$\frac{\langle \sigma v \rangle_T}{v_T} = \left(\frac{4}{\pi} \right)^{1/2} \int_0^\infty \sigma(E) x e^{-x} dx, \quad (22)$$

where $x = E/kT$. Since $(\Gamma_n \Gamma_\gamma / \Gamma D)_i$ in Eq. (20) is a slowly varying function of E , a first approximation to Eq. (20) is obtained by evaluating it at $E = kT$. Then Eq. (22) becomes $\langle \sigma v \rangle_T / v_T \approx (4/\pi)^{1/2} \sigma(kT)$,

with which it is easy to determine the constants C_1 to C_5 from the empirical data. To determine C_1 and C_2 , the (n, γ) reactions leading to odd-odd compound nuclei for which $\Delta_{o.o.} \approx 0$ were used. Then the reactions leading to the odd-odd compound nuclei for which $\Delta_{o.o.} \neq 0$ were used to determine C_3 . With C_1 , C_2 , and C_3 determined, the reactions leading to even-odd and odd-even nuclei were used to determine C_4 . Finally, C_5 was determined using reactions leading to even-even compound nuclei. Once first approximations to the empirical constants are available, it is possible to integrate Eq. (22) numerically, taking into account the variation of $(\Gamma_n \Gamma_\gamma / \Gamma D)_i$ with energy. Final values for the constants are obtained by adjusting to a best fit to the empirical values for $\langle \sigma v \rangle_T / v_T$. These are $C_1 = 3.72$, $C_2 = 0.286 \text{ MeV}^{-1/2}$, $C_3 = 1.8$, $C_4 = 3.8$, and $C_5 = 1.3$, so that Eq. (12) becomes

$$\begin{aligned} \log_{10}(\Gamma_\gamma/D) &= \log_{10} T_\gamma - 0.80 \\ &= -3.72 - 3.33 \log_{10} A_C + 0.286 (A_C B')^{1/2} \\ &\quad + 3.95 (A_C B')^{-1/2}. \end{aligned} \quad (23)$$

Except for the dependence on A_C , this equation is very similar to that used by Wagoner, Fowler, and Hoyle.¹⁷ It gives a superior fit to the experimental results for (n, γ) reactions. Certain numerical examples are given in Table II.

Figure 2 shows the ratio of the calculated $\langle \sigma v \rangle_T / v_T$, using the adjusted constants to the experimental values at $kT = 30 \text{ keV}$. For $A \leq 176$, six ratios lie outside the range 0.4 to 2.5. There were four reactions leading to even-odd compound nuclei for which the first excited state of only one of the bracketing even-even nuclei was known: $^{96}\text{Zr}(n, \gamma)$ - ^{97}Zr , $^{100}\text{Mo}(n, \gamma)$ - ^{101}Mo , $^{130}\text{Te}(n, \gamma)$ - ^{131}Te , and $^{154}\text{Sm}(n, \gamma)$ - ^{155}Sm . All four cases are poorly fitted. Moreover, our treatment has included the effects of nuclear deformation only in a very crude way. This seems to result in satisfactory results for $A \leq 176$

TABLE II. Numerical examples.

Reaction	A_C	Bracketing even-even nuclei	B (MeV)	$\delta(N)$ (MeV)	$\sum_{i=1}^M \frac{E_{e.e.}^i(i)}{-\delta(N)}$ (MeV) (Ref. a)	Δ (MeV)	$B' = B - \Delta$ (MeV)	Γ_γ/D
$^{28}\text{Si}(n, \gamma)$ - ^{29}Si	29	^{28}Si , ^{30}Si	8.475	0.64	1.26	4.73	3.74	5.9×10^{-6}
$^{50}\text{V}(n, \gamma)$ - ^{51}V	51	^{50}Ti , ^{52}Cr	11.05	0.54	0.76	3.47	7.68	2.7×10^{-4}
$^{51}\text{V}(n, \gamma)$ - ^{52}V	52	^{50}Ti , ^{52}Ti , ^{52}Cr , ^{54}Cr	7.31	0.53	0.68	1.23	6.08	7.5×10^{-5}
$^{53}\text{Cr}(n, \gamma)$ - ^{54}Cr	54	^{54}Cr	9.72	0.52	0.31	3.90	5.82	6.3×10^{-5}
$^{100}\text{Ru}(n, \gamma)$ - ^{101}Ru	101	^{100}Ru , ^{102}Ru	6.806	0.34	0.16	1.59	5.21	2.2×10^{-4}

^a M is 1 for even-even compound nuclei, 2 for even-odd or odd-even nuclei, and 4 for odd-odd nuclei.

through the adjustment of the five free parameters but may be the cause of the divergence for $A > 176$. The poor fit in this region may also be related to the closure of a proton shell as well as a neutron shell at ^{208}Pb . The effects of this closure begin to be appreciable at $A \sim 173$ in the excitation of the first excited state.

IV. CALCULATED REACTION RATES

For our final calculations of cross sections for reactions of interest to us as a function of energy, we returned to Eq. (1). Transmission functions for α , p , and n channels were determined using Eq. (3) and the parameters of Table I. The transmission function for the γ channel was determined from Γ_γ/D as discussed in Sec. III. The spin and parity of the ground states of the target and residual nuclei were taken from *Nuclear Data Sheets*.¹⁸ The inelastic scattering channels were neglected. The reaction rates as a function of temperature were then obtained from Eqs. (18) and (22). The results were fitted to expressions of the form

$$N_A \langle \sigma v \rangle_T = \text{const} \times e^{-E_{\text{th}}/kT} \text{ cm}^3 \text{ g}^{-1} \text{ sec}^{-1}, \quad (24)$$

where N_A is Avogadro's number.¹⁹ The empirical energy E_{th} is an effective threshold energy for the reaction. For exoergic reactions, it is usually somewhat less than the Coulomb barrier in the incident channel. For endoergic reactions with negative Q values, E_{th} differs from $|Q|$ somewhat because of Coulomb effects in the incoming and out-

going channels. For (n, γ) reactions it is generally found that $E_{\text{th}} = 0$ and $\langle \sigma v \rangle_T = \text{const}$ over a limited range of temperature. For convenience, Eq. (24) has been transformed to

$$\log_{10} N_A \langle \sigma v \rangle_T = \log_{10} B_1 + B_2 \left(\frac{1}{4} - 1/T_9 \right), \quad (25)$$

where $B_1 = N_A \langle \sigma v \rangle_T$ at $T_9 = 4$ in the middle of the temperature range of interest and $B_2 = 5.04 E_{\text{th}}$ for E_{th} in MeV. Equation (25) fits the calculated values for $N_A \langle \sigma v \rangle_T$ to within approximately 20% over the range $3 \leq T_9 \leq 6$. The fit is good to a factor of 2 down to $T_9 = 2$. The calculated results for certain reactions of astrophysical interest are given in Table III. Table IV shows a comparison of the calculated reaction rates with available experimental rates²⁰ and with those calculated by Truran, Cameron, and Gilbert (TCG).¹² Our calculated rates involving only particle channels are within a factor of 2 of the observed rates, whereas those involving γ rays are within a factor of 3. The main uncertainty in the (p, γ) rates comes from the γ channels, since the proton channels are not very sensitive to the radius used.

To determine an experimental rate at a given temperature when charged particles are involved, it is necessary to know the properties of all resonances within the width ΔE_0 around the effective thermal energy E_0 , where²²

$$E_0 = 0.122 (Z_1^2 Z_0^2 A T_9^2)^{1/3} \text{ MeV},$$

$$\Delta E_0 = 0.237 (Z_1^2 Z_0^2 A T_9^5)^{1/6} \text{ MeV},$$

TABLE III. Constants for the reaction rates in $\text{cm}^3 \text{ g}^{-1} \text{ sec}^{-1}$.

Reaction	B_1	B_2	$E_{\text{th}}/B_2/5.04$ (MeV)	Q of the reaction (MeV)
$^{27}\text{Al}(p, \alpha)$	3.6×10^5	6.7	1.33	1.6
$^{31}\text{P}(p, \alpha)$	6.9×10^5	7.3	1.44	1.9
$^{31}\text{P}(p, \gamma)$	1.09×10^4	3.86	0.77	8.9
$^{34}\text{S}(p, \gamma)$	1.43×10^4	3.31	0.66	6.4
$^{41}\text{Ca}(\alpha, \gamma)$	6.6	17.6	3.0	6.3
$^{42}\text{Ca}(\alpha, \gamma)$	1.14×10	16.7	3.0	8.0
$^{42}\text{Ca}(\alpha, p)$	1.76×10	20.6	4.0	-2.3
$^{42}\text{Ca}(\alpha, n)$	7.9	27.0	5.4	-5.2
$^{43}\text{Ca}(n, \gamma)$	7.8×10^6	0.0	0.0	6.7
$^{44}\text{Ca}(p, \gamma)$	5.7×10^4	5.35	1.0	6.9
$^{44}\text{Ca}(p, n)$	3.7×10^3	22	4.4	-4.4
$^{44}\text{Sc}(p, \gamma)$	3.2×10^4	6.14	1.2	8.5
$^{44}\text{Sc}(n, \gamma)$	1.3×10^7	0.0	0.0	11.3
$^{44}\text{Sc}(p, n)$	4.4×10^5	8.3	1.6	-0.9
$^{44}\text{Ti}(\alpha, p)$	8.9	23	4.6	-0.5
$^{44}\text{Ti}(n, \gamma)$	6.6×10^6	0.0	0.0	9.4
$^{45}\text{Sc}(p, \gamma)$	1.3×10^5	6	1.2	10.4
$^{45}\text{Sc}(p, n)$	9.2×10^4	14.3	2.8	-2.8
$^{45}\text{Ti}(n, \gamma)$	1.5×10^7	0.0	0.0	13.2
$^{52}\text{Cr}(p, \gamma)$	1.86×10^4	6.44	1.28	6.6

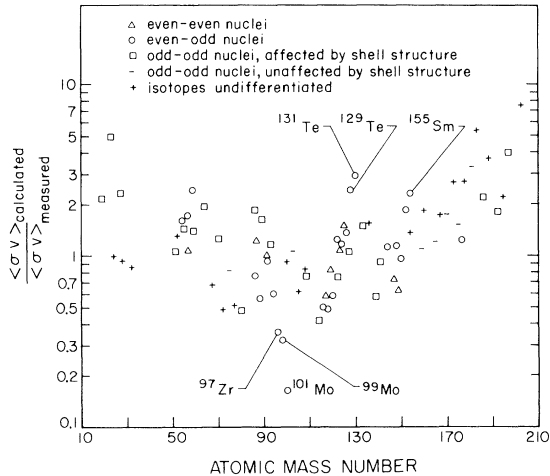


FIG. 2. Comparison of the calculated $\langle \sigma v \rangle_T$ values for (n, γ) reactions [Macklin and Gibbons (Refs. 1 and 2)]. For $A < 176$ there are about 70 measured cross sections. For six of these the calculated value is outside a factor of 2.5 from the measured value. The atomic-mass numbers refer to the compound nuclei. The nuclei indicated are the compound nuclei.

Z_0 and Z_1 are, respectively, the charge numbers of the target nucleus and of the incident particle, and A is the reduced mass. E_0 is at least 1 MeV for protons and 2 MeV for α particles. Only very few reactions have been studied carefully enough in the mass range of main interest to us, $Z_0 \geq 20$. This is why Table IV is rather limited and actually involves target nuclei with somewhat smaller Z_0 than we were mainly interested in.

In evaluating the accuracy of the calculations, it is useful to bear in mind the range of energies involved. For instance, for a proton incident on ^{40}Ca at $T_9 = 2$, $E_0 = 1$ MeV, and $\Delta E_0 = 1$ MeV. Thus an average is taken over an energy range larger, in general, than 1.0 MeV. Furthermore, there are usually at least three J values involved. After averaging over $\Delta E_0 \geq 1$ MeV and over three J values, fluctuations in the level density are not expected to lead to order-of-magnitude errors in compound nuclei with $Z \geq 20$.

It is true that Table IV is somewhat meager. We, however, included all reaction rates available to us for which there appeared to be enough data over the energy range of interest and which were in the proper mass range. Finally, it must be noted that *none* of the disposable constants were fitted to the data included in Table IV. The constants were all fitted through comparison with the 70 or so measured (n, γ) cross sections.

Table V shows a comparison of the calculated rates around atomic mass number 44 to those calculated by TCG.²¹ In their calculations TCG²¹ approximated the effect of excited states in the target nucleus by multiplying the right-hand side of Eq. (1) by $(2I_T + 1)/\omega_T$, where I_T , designated by I in Eq. (1), is the spin of the ground state of the target nucleus and ω_T is the partition function for the target nucleus (including the excited states). They imply that inelastic scattering can be approximated by

TABLE IV. Comparison of calculated and measured rates ($\text{cm}^3 \text{g}^{-1} \text{sec}^{-1}$).

Reaction	T_9	Experimental (Ref. 20)	These calculations	TCG (Ref. 21)
$^{27}\text{Al}(p, \alpha)$	3	1.1×10^5	9.6×10^4	9.6×10^4
	5	4.7×10^5	7.8×10^5	4.1×10^5
$^{31}\text{P}(p, \alpha)$	3	1.6×10^5	1.7×10^5	1.5×10^5
	5	7.8×10^5	1.6×10^6	7.2×10^5
$^{31}\text{P}(p, \gamma)$	3	2.6×10^3	5.2×10^3	9.0×10^3
	5	5.9×10^3	1.7×10^4	2.4×10^4
$^{34}\text{S}(p, \gamma)$	3	2.4×10^3	7.6×10^3	9.0×10^3
	5	6×10^3	2.1×10^4	3.4×10^4
$^{52}\text{Cr}(p, \gamma)$	3	1.5×10^3	5.4×10^3	6.0×10^3
	5	1.1×10^4	3.9×10^4	5.4×10^4

the partition function. The approximation is expected to be good only if the denominator of Eq. (1) is dominated by the entrance channel. If it is dominated by any other channel, the factor $(2I_T + 1)/\omega_T$ will be an overcorrection. This correction is seen to introduce a factor of up to 4 when ^{44}Sc is the target nucleus. When this is taken into account, the two sets of calculations seem to agree very well except for $^{43}\text{Sc}(p, n)$ and $^{43}\text{Ca}(n, \gamma)$. In the latter case, the difference is probably mainly due to Γ_γ/D . In the $^{45}\text{Sc}(p, n)$ case, however, the source of the disagreement is harder to trace. Most of the present calculations give larger reaction rates, mainly because of the inclusion of the reflection factor, f , in Eq. (4).

Another effect of the uncertainty of the spin and parity can be studied by calculating reaction rates

TABLE V. Comparison of calculated rates ($\text{cm}^3 \text{g}^{-1} \text{sec}^{-1}$).

Reaction	T_9	These calculations	TCG (Ref. 21)	TCG $\times \omega_T/(2I_T + 1)$
$^{41}\text{Ca}(\alpha, \gamma)$	3	2.4×10^{-1}	1.3×10^{-1}	1.3×10^{-1}
	5	5.4×10	3.5×10	3.5×10
$^{42}\text{Ca}(\alpha, \gamma)$	3	3.9×10^{-1}	2.5×10^{-1}	2.5×10^{-1}
	5	9.6×10	5.0×10	6.0×10
$^{42}\text{Ca}(\alpha, p)$	3	2.7×10^{-1}	1.3×10^{-1}	1.3×10^{-1}
	5	2.5×10^2	1.2×10^2	1.5×10^2
$^{42}\text{Ca}(\alpha, n)$	3	4.2×10^{-2}	1.6×10^{-2}	1.6×10^{-2}
	5	1.9×10^2	8.5×10	1.0×10^2
$^{43}\text{Ca}(n, \gamma)$	3	7.4×10^6	1.4×10^6	1.8×10^6
	5	8.2×10^6	1.4×10^6	2.2×10^6
$^{44}\text{Ca}(p, \gamma)$	3	2.0×10^4	2.2×10^4	2.4×10^4
	5	1.1×10^5	1.2×10^5	1.7×10^5
$^{44}\text{Ca}(p, n)$	3	5.0×10	2.2×10	2.4×10
	5	5.0×10^4	2.1×10^4	3.1×10^4
$^{44}\text{Sc}(p, \gamma)$	3	1.04×10^4	3.1×10^3	9.6×10^3
	5	7.0×10^4	1.3×10^4	6.3×10^4
$^{44}\text{Sc}(n, \gamma)$	3	1.1×10^7	3×10^6	9.0×10^6
	5	1.2×10^7	3×10^6	1.5×10^7
$^{44}\text{Sc}(p, n)$	3	8.4×10^4	2.2×10^4	6.6×10^4
	5	1.3×10^6	1.9×10^5	9.6×10^5
$^{45}\text{Sc}(p, \gamma)$	3	3.8×10^4	2.8×10^4	3.6×10^4
	5	2.7×10^5	1.4×10^5	2.4×10^5
$^{45}\text{Sc}(p, n)$	3	1.4×10^3	3.0×10^3	3.6×10^3
	5	5.5×10^4	2.2×10^5	3.6×10^5
$^{44}\text{Ti}(\alpha, p)$	3	1.2×10^{-1}	1.1×10^{-1}	1.1×10^{-1}
	5	1.5×10^2	8.0×10	1.0×10^2
$^{44}\text{Ti}(n, \gamma)$	3	6.1×10^6	2.9×10^6	2.9×10^6
	5	6.9×10^6	3.5×10^6	4.4×10^6
$^{45}\text{Ti}(n, \gamma)$	3	1.4×10^7	6.6×10^6	1.1×10^7
	5	1.6×10^7	6.6×10^6	1.3×10^7

on the assumption that the target and residual nuclei, and the incoming and outgoing particles all have zero spin and the required parity. Equation (1) then becomes Eq. (20).

In most cases, Eq. (20) is a very good approximation to Eq. (1). However, when neither α nor α' is the main open channel, Eq. (20) implies that the leading term in Eq. (1) would be that for $l=0$ and would contain

$$\frac{T_0(\alpha)T_0(\alpha')}{T_0(\alpha)+T_0(\alpha')+T_0(\text{main channel})} \approx \frac{T_0(\alpha)T_0(\alpha')}{T_0(\text{main channel})} \quad (26)$$

If there were a large spin difference between the residual nucleus for the main channel compared with the α and α' channels, Eq. (1) would correctly give the right-hand side of Eq. (26) as

$$\frac{T_0(\alpha)T_0(\alpha')}{T_0(\alpha)+T_0(\alpha')+T_{\Delta I \pm 1/2}(\text{main channel})} \quad (26')$$

in the case $i = \frac{1}{2}$ for a neutron or proton in the main channel. The spin difference between the main channel and the channels involving the target and residual nuclei is taken as ΔI , assuming for illustration that these nuclei have the same spin.

Consider the case for the $^{41}\text{Ca}(\alpha, \gamma)^{45}\text{Ti}$ reaction in which the ground states of both ^{41}Ca and ^{45}Ti have $I^\pi = \frac{7}{2}^-$. Thus for the dominant partial wave, $l=0$, the compound nucleus also has $J^\pi = \frac{7}{2}^-$. At high enough temperatures the endoergic reactions $^{41}\text{Ca}(\alpha, n)^{44}\text{Ti}$ and $^{41}\text{Ca}(\alpha, p)^{44}\text{Sc}$ compete with $^{41}\text{Ca}(\alpha, \gamma)^{45}\text{Ti}$. Thus, the leading term in Eq. (20) is proportional to

$$\frac{T_0(\alpha)T(\gamma)}{T_0(\alpha)+T(\gamma)+T_0(n)+T_0(p)} \approx \frac{T_0(\alpha)T(\gamma)}{T_0(n)} \quad (27)$$

using T 's rather than (Γ/D) 's for easy comparison with Eq. (1). The right-hand side of Eq. (27) follows, since $T_0(n)$ is considerably larger than the other T 's. However, the ground state of ^{44}Ti has $I^\pi = 0^+$ and that of ^{44}Sc has 2^+ . Thus the leading term is given correctly in accordance with the conservation of angular momentum and parity by Eq. (1) as proportional to

$$\frac{T_0(\alpha)T(\gamma)}{T_0(\alpha)+T(\gamma)+T_3(n)+T_1(p)} \approx \frac{T_0(\alpha)T(\gamma)}{T_0(\alpha)+T_1(p)} \quad (28)$$

where the right-hand side of Eq. (28) follows, since

$$T(\gamma)+T_3(n) < T_0(\alpha)+T_1(p) \ll T_0(n) \quad (28')$$

The cross section calculated for $^{41}\text{Ca}(\alpha, \gamma)^{45}\text{Ti}$ by the use of Eq. (20) is too small by a factor of 3 relative to the cross section from Eq. (1). This is

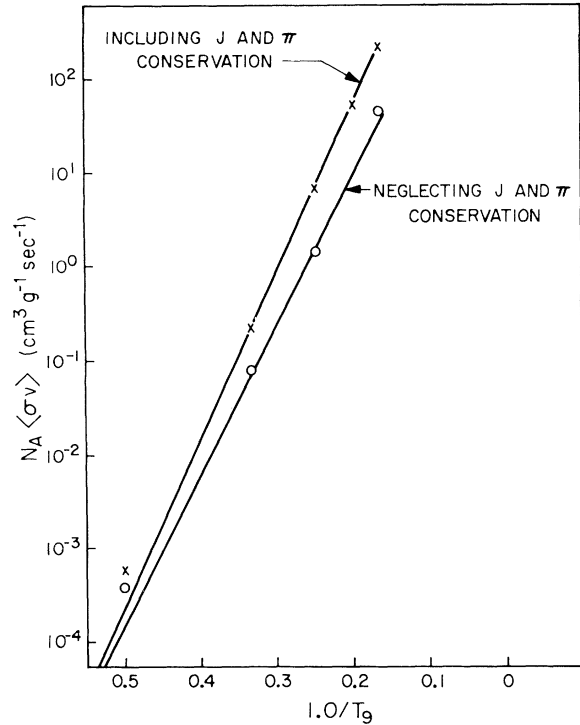


FIG. 3. Reaction rate for the reaction $^{41}\text{Ca}(\alpha, \gamma)^{45}\text{Ti}$ which must compete at high temperatures with $^{41}\text{Ca}(\alpha, n)^{44}\text{Ti}$ (I^π of ^{41}Ca is $\frac{7}{2}^-$, I^π of ^{44}Ti is 0^+). Neglect of the conservation of spin and parity is seen to decrease the cross section by a factor 3 or so. This will be the case only when there are large differences between the spins of the ground states of the nuclei involved in open channels. Our fitting formula (straight line) fits the calculated points when $1/T_9 \lesssim 0.04$ or $T_9 \gtrsim 2.5$.

illustrated in Fig. 3. Similarly, for $^{44}\text{Sc}(p, \gamma)^{45}\text{Ti}$ the factor is 10.

If low-lying excited levels had a spin different from the ground state by $\Delta I \leq 2$, inaccuracies have resulted from our neglecting them. Consider, for example, that the reaction rate for a $^AZ(\alpha, p)$ reaction on an even- Z even- N nucleus ($I^\pi = 0^+$ for the target nucleus) is to be calculated. Assume that the $^{A+3}(Z+1)$ nucleus (the residual nucleus) has $I^\pi = \frac{7}{2}^-$. The conservation of total spin will then eliminate all combinations such as $T_0(\alpha)T_0(p)$ or $T_1(\alpha)T_1(p)$ and allow only the smaller combinations, $T_0(\alpha)T_3(p)$, $T_1(\alpha)T_2(p)$, ..., $T_3(\alpha)T_0(p)$. However, if the first excited level of $^{A+3}(Z+1)$ is a low-lying state with $I^\pi = \frac{1}{2}^+$, combinations such as $T_0(\alpha)T_0(p)$, $T_1(\alpha)T_1(p)$ would be allowed again and could enhance the cross sections by 1 order of magnitude. From shell-model calculations,²³ levels with $I^\pi = \frac{7}{2}^-$ are expected to occur in the mass range of interest here ($A \approx 44$). However, no $I^\pi = \frac{1}{2}^+$ level is expected to be at low excitation. The enhancement is then not expected to be large (prob-

ably smaller than 30%). In any case, when sufficient experimental data on spins and parities are available, Eq. (1) should be used in preference to Eq. (20). The effects of excited states and of the conservation laws are then properly included. Only in the case of reactions involving γ channels is it sometimes warranted to resort to Eq. (20), and then it must be realized that the errors can be large if there are open channels whose spin differs from the spins of the channels of interest by $\Delta I \geq 2$.

In conclusion, it is our considered opinion that

the prescription for calculation of reaction rates discussed in this paper is straightforward and easily adaptable to computer calculations, and that it produces results well within the uncertainties in present experimental determinations. It has the advantage of being simpler to carry out than other methods of similar accuracy and of directly relating, through the equivalent square well, the calculations of particle channels to currently fashionable optical models.

*Work supported in part by the National Science Foundation (GP-15911, GP-9114, and GP-19887) and the Office of Naval Research [Nonr-220(47)].

†Now at Département de Physique, Université de Montréal, Montréal, Canada.

¹R. L. Macklin and J. H. Gibbons, *Rev. Mod. Phys.* **37**, 166 (1965).

²R. L. Macklin and J. H. Gibbons, *Astrophys. J.* **150**, 721 (1967).

³G. Michaud and W. A. Fowler, to be published.

⁴G. Michaud, L. Scherk, and E. W. Vogt, *Phys. Rev. C* **1**, 864 (1970).

⁵W. Hauser and H. Feshbach, *Phys. Rev.* **87**, 366 (1952); E. Vogt, in *Advances in Nuclear Physics*, edited by M. Baranger and E. Vogt (Plenum Press, Inc., New York, 1968), Vol. 1, p. 261.

⁶E. Vogt, *Rev. Mod. Phys.* **34**, 723 (1962).

⁷These terms are defined by Vogt, Ref. 6, and are normally included in the expressions from which our Eq. (3) originates.

⁸J. M. Blatt and V. F. Weisskopf, *Theoretical Nuclear Physics* (John Wiley & Sons, Inc., New York, 1952).

⁹B. B. Kinsey, *Handbuch der Physik* (Springer-Verlag, Berlin, Germany, 1957), Vol. XL, p. 202.

¹⁰J. Morgenstern, R. Alves, S. de Barros, J. Julien, and C. Samour, in *Proceedings of the Conference on Neutron Cross Sections and Technology, Washington, D. C., 1968*, edited by D. T. Goldman (National Bureau of Standards Special Publication No. 299, 1968), p. 867.

¹¹H. A. Bethe, *Rev. Mod. Phys.* **9**, 69 (1937).

¹²G. Michaud, Ph. D. thesis, California Institute of Technology, 1970 (unpublished).

¹³H. Hurwitz and H. A. Bethe, *Phys. Rev.* **81**, 898 (1951); T. D. Newton, *Can. J. Phys.* **34**, 804 (1956).

¹⁴W. A. Fowler and F. Hoyle, *Astrophys. J. Suppl.* **9**, (No. 91) 201 (1964).

¹⁵H. W. Newson, in *Proceedings of the International Conference on the Study of Nuclear Structure with Neutrons, Antwerp, Belgium, 1965*, edited by M. Nève de Mévergnies, P. Van Assche, and J. Vervier (North-Holland Publishing Company, Amsterdam, The Netherlands, 1966).

¹⁶E. J. Campbell, H. Feshbach, C. E. Porter, and V. F. Weisskopf, Massachusetts Institute of Technology, Technical Report No. 73, 1960 (unpublished).

¹⁷R. V. Wagoner, W. A. Fowler, and F. Hoyle, *Astrophys. J.* **148**, 3 (1967).

¹⁸*Nuclear Data Sheets*, compiled by K. Way *et al.* (Printing and Publishing Office, National Academy of Sciences - National Research Council, Washington, D. C.), Vols. 1-6.

¹⁹It is customary to calculate $N_A \langle \sigma v \rangle_T$ from the experimental or theoretical dependence of the cross section on energy. When this quantity is multiplied by $n_1/N_A = \rho X_1/A_1$, the reaction rate per second per target nucleus is obtained. In this multiplying factor, n_1 is the number density per cm^3 of the incident particles with which the target nucleus interacts, ρ is the density in g cm^{-3} of the medium, X_1 is the fraction of the total mass contributed by the incident particles, and A_1 is their atomic mass.

²⁰W. A. Fowler, unpublished.

²¹J. W. Truran, A. G. W. Cameron, and A. Gilbert, *Can. J. Phys.* **44**, 563 (1966).

²²E. M. Burbidge, G. R. Burbidge, W. A. Fowler, and F. Hoyle, *Rev. Mod. Phys.* **29**, 547 (1957).

²³M. A. Preston, *Physics of the Nucleus* (Addison-Wesley Publishing Company, Inc., Reading, Massachusetts, 1962), p. 150.